Near-surface oceanic temperature gradients

This discussion document is to provide an explanation of the cartoon of near-surface temperature gradients that is on the GHRSST web pages (Figure 1), and which receives frequent attention, giving rise to a number of queries.

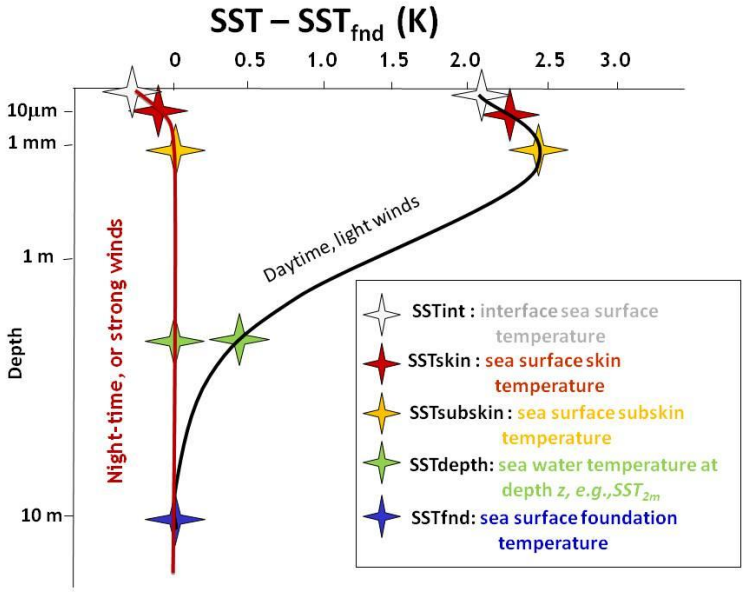

Figure 1. Cartoon of near-surface temperature gradients. The numbers on the axes are for guidance only and to not represent rigorously derived scales. Variability exists in both the temperature and depth scales.

Near-surface temperature gradients on the aqueous side of the air-sea interface result from three different processes: (1) the absorption of insolation in the first meters, (2) the heat loss to the atmosphere (by emission of thermal radiation originating from within the first millimeter and thermal conduction there), and (3) the levels of subsurface turbulent mixing. The following discussion is presented in terms of a **mean skin layer**, where mean indicates averaging over length and spatial scales that are long compared to those of the turbulent eddies in the ocean that erode the skin layer. This is certainly the case for satellite measurements which are spatial averages over typically 1km^2 or more, and similarly for ship-board radiometers where the combination of a footprint size of several m^2 and a finite integration time tend to smear the signals of the structure of the surface thermal skin.

Absorption of insolation in the first meters and resulting temperature gradient: The solar radiation that penetrates the air-sea interface is mostly absorbed, heating the water over depths of several meters or more (Figure 2). Since the ocean is nearly always warmer than the overlying atmosphere, there is heat flow from the ocean to the air above.

Heat loss in the thermal skin layer: The sign of the temperature gradient in approximately the first millimeter is nearly always such that the surface is cooler than the underlying water and here the conductive heat flow supplies energy for the heat loss to the atmosphere, both the radiant (net infrared) heat loss and the sensible and latent heat losses. The sensible and latent heat losses are removed from the ocean-atmosphere interface by turbulent eddies in the atmospheric boundary

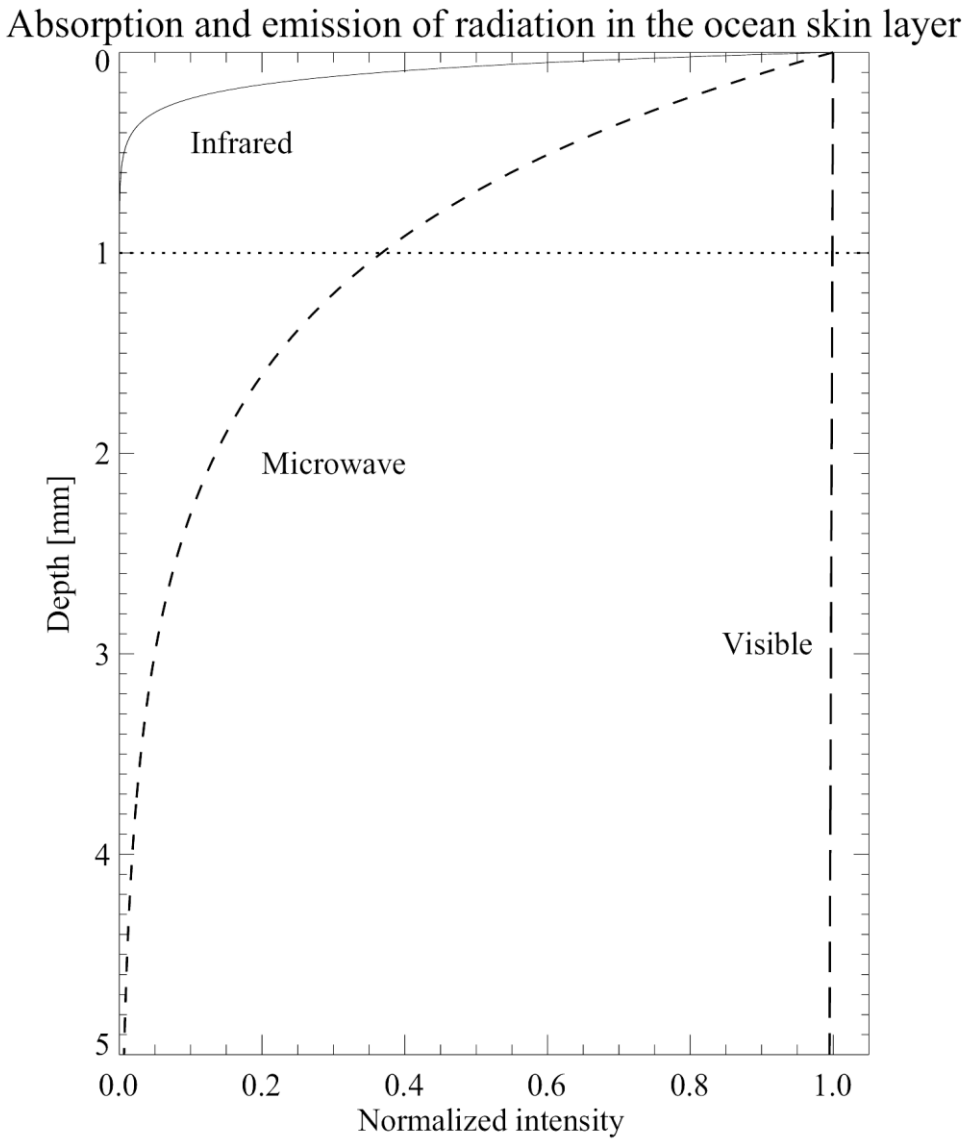

Figure 2. Profiles of normalized intensity of radiation through the upper 5mm of the ocean surface for visible, infrared and microwave radiation normally incident at the sea surface. The Beer-Lambert's Law absorption coefficients are: 1 m^{-1} in the visible, 10^{-4} m^{-1} in the infrared, and 10^{-3} m^{-1} in the microwave. By Kirchhoff's Law, the emission coefficient equals the absorption coefficient for local thermodynamic equilibrium.

layer. The thin aqueous layer that supports the temperature gradient is referred to as the "thermal skin layer" and even though it is statically unstable (colder water overlying warmer water) it is hindered by the viscosity of the water from convecting to attain static stability.

Considering the absorption of radiation by the sea, Beer-Lambert's Law describes how the intensity, *I*, of an electromagnetic wave decays exponentially within a medium as a function of the path length from the interface (*z*):

$$I(\lambda, z) = I_0(\lambda)\, e^{-\alpha(\lambda)z} \qquad (1)$$

where α is a wavelength (λ) dependent attenuation coefficient. The penetration depth, δ(λ), is 1/α(λ) which is referred to as the electromagnetic skin depth and gives the distance along the path of propagation for the intensity to drop to 1/e of its value at the interface. For infrared wavelengths, δ is typically a few tens of μm (Bertie and Lan 1996), and for microwaves, at the frequencies used to measure SST (Wilheit et al. 1980; Gentemann et al. 2010), it is typically a few mm (Swift 1980). In the visible part of the spectrum δ depends of on the turbidity of the water but away from the coast it is typically a meter or more.

The emission of radiation by the sea surface is also described by Beer-Lambert's Law with the absorption coefficient being replaced by an emission coefficient. And by Kirchhoff's Law, under conditions of thermal equilibrium, the emission and absorption coefficients are identical. Thus, we can interpret the Fig. 2 as an emission profile as well as an absorption profile. The spectral composition of the emitted radiation $I_0(\lambda)$ is given by Planck's equation.

Figure 2 illustrates that the emission measured in the infrared has its origins in the thermal skin layer (except for situations where the skin layer is very thin), and that a portion of the microwave emission originates from below the skin layer. In the visible part of the spectrum, emission from the sea surface is essentially zero. The same intensity curves apply for the absorption of radiant energy in the upper ocean. Estimates of the average thickness of the thermal skin layer vary, ranging from a few mm (Katsaros et al. 1977) to a few tenths of a mm, or less (Hanafin 2002; Hanafin and Minnett 2001), and this is to be expected as the thermal skin layer is a dynamic feature being eroded by turbulence below (e.g. Soloviev and Schlüssel 1994). Thus, nearly all of the infrared radiation from the sun and atmosphere that is incident at the sea surface is absorbed within the thermal skin layer, while some of microwave energy penetrates the skin layer. In the visible, for an absorption coefficient of 1 m^{-1} about 99.9% of the incident energy penetrates the uppermost millimeter of the ocean surface. These curves are for normal incidence and emission, and for a slant path propagation the vertical scale should be reduced accordingly (i.e. by the cosine of the zenith angle of propagation).

Thus, at infrared wavelengths the electromagnetic skin layer is entirely embedded in the thermal skin layer, and in the microwave, at frequencies where SST is derived, the thermal and electromagnetic skin depths are comparable and the microwave electromagnetic skin depth can extend into the sub-skin regime of the ocean. The infrared radiance emitted by the ocean surface, some of which in selected spectral intervals is measured by satellite radiometers and used to derive estimates of SST, has its origin in the thermal skin layer of the ocean and not in

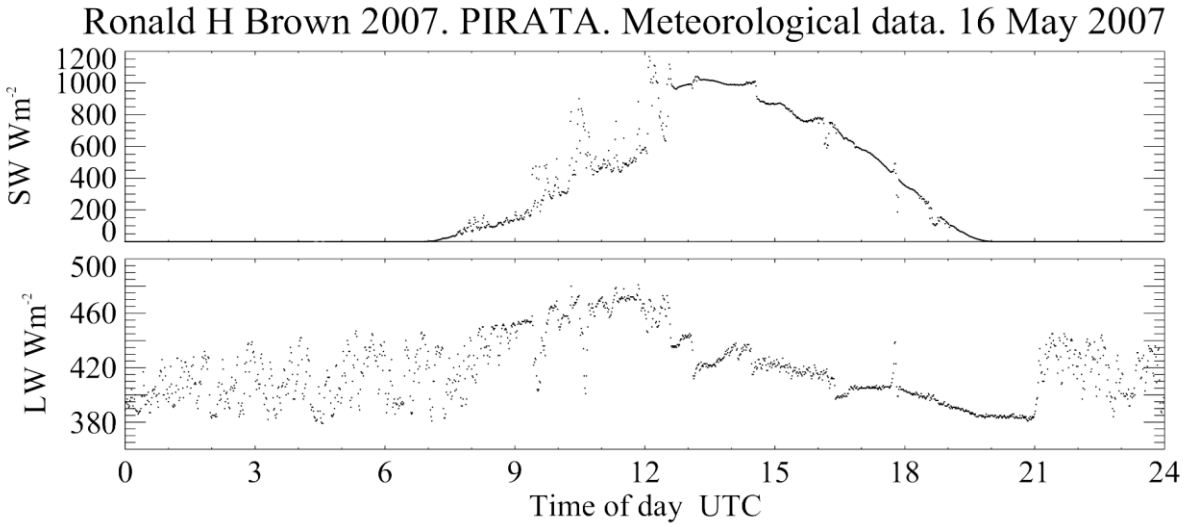

Figure 3. An example of time series of incident solar (shortwave - SW) radiation and thermal infrared (longwave - LW) radiation incident at the sea surface for a 24 h period measured on the NOAA Ship *Ronald H Brown* in the tropical Atlantic Ocean (~15°N, ~23°W) on May 16th, 2007. The shortwave includes radiation in the wavelength range of 0.285 to 2.8μm and the long wave 3.5 to 50 μm. The shortwave signal reveals the effect of the change in solar zenith angle during the day, with modulation caused by clouds. Similarly, the long wave signal is modulated by clouds, but they cause an effect generally in the opposite sense to that in the shortwave.

the body of the water below which is what is measured by in situ thermometers, and has been for many decades (Kent and Taylor 2006). The SST measured by infrared radiometers is often referred to as the skin SST (SST_{skin}). The subsurface temperature is frequently called the 'bulk SST' although it is better practice to qualify the subsurface temperature by giving the depth of the measurement (T_z) (Donlon et al. 2007).

On a clear day in the tropics the insolation reaching the sea-surface can peak at about 1000 Wm^{-2} (Figure 3) which means that about 1 Wm^{-2} is absorbed in the uppermost millimeter. This is to be contrasted with the total incident infrared emission, typically in the range of 300-500 Wm^{-2} depending on cloud cover and the amount of water vapor in the atmosphere, which is all absorbed in the less than the uppermost millimeter.

The relationship between the temperature in the thermal skin layer and the sub-skin temperature just below the surface is reasonably well behaved (Minnett et al. 2011), having an asymptote of about -0.13K at high winds and exceeding -0.6K at low winds. The relationship with deeper bulk temperature, at depths of tens of centimetres to a few metres where many subsurface temperature measurements are taken, is the same on average during the night, and during the day for surface wind speeds of >~6ms^{-1} (Donlon et al. 2002). In conditions of

moderate to high wind speeds the heat is mixed vertically throughout the mixed layer by wind-generated turbulence and wave effects.

Under low winds the relationship between SST_{skin} and T_z is very variable - vertically, horizontally and temporally (Minnett 2003; Ward 2006; Gentemann and Minnett 2008). In conditions of low wind speed, the heat generated in the upper ocean by the absorption of solar radiation is not well mixed through the surface layer, but causes thermal stratification with temperature differences between the uppermost layer of the ocean and the water below. There is a strong diurnal component to the magnitude of these temperature gradients, as well as a dependence on cloud cover which modulates the insolation and, importantly, wind speed which influences the turbulent mixing (e.g. Price et al. 1986; Fairall et al. 1996; Gentemann and Minnett 2008). The difference between the skin temperature and that measured by a sub-surface, in situ thermometer in the presence of diurnal heating is strongly dependent on the depth of the sub-surface measurement, and can exceed 4K. When the amplitude of the diurnal heating at the sea surface is determined by comparisons with SSTs measured during the previous night, multiple cases of amplitudes in excess of 6K have been identified (Gentemann et al. 2008). Even in the presence of large diurnal heating that can cause the SST_{skin} to be greater than T_z, the thermal skin layer, sustained by heat loss to the atmosphere, results in the SST_{skin} being cooler than the sub-skin temperature (Minnett 2003; Minnett et al. 2011). The variability of near-surface temperature gradients can be large compared to the accuracies of SST needed for climate research (e.g. Ohring et al. 2005), and thus the effects of the thermal skin layer and diurnal heating must be taken into account when generating CDRs of SST. For this reasons, a SST foundation temperature is defined and suggested for use in climate applications.

In reality the thermal properties of the surface of the ocean are very variable and are driven by turbulence. While the augments above are in terms of the mean skin layer, the embedded hyperlinks will take you to video clips of the water surface in a wind-wave tank taken with an infrared imager. The dimensions of the surface are about 30x40cm in each image and the colors indicate the skin temperatures. In each case the airflow is from the lower left to the upper right. The air-sea temperature difference is -15K (air cooler than water) which is large compared to most situations in nature, but was imposed here to ensure a clear signal in the infrared imagery. The loop with coherent structures is for a wind speed of 2 ms^{-1} (http://www.rsmas.miami.edu/personal/pminnett/Skin_layer_video/CS031.AVI) and the warm patches are the tops of the turbulent eddies bringing warmer subskin water into the skin layer. The colder filaments are where surface convergence is concentrating the water than has been in the skin layer longest and is therefore cooler. The other loop is for a wind speed of 9 ms^{-1} (http://www.rsmas.miami.edu/personal/pminnett/Skin_layer_video/CS037.AVI) and thus breaking waves are present. The structures are smaller and less coherent in space and time, but the range of skin temperatures is comparable to the lower wind speed case where there are no breaking waves.

Please direct corrections, comments and recommendations for improvements to Peter Minnett (pminnett@rsmas.miami.edu)

References

Bertie, J. E. and Z. Lan, 1996: Infrared Intensities of Liquids XX: The Intensity of the OH Stretching Band of Liquid Water Revisited, and the Best Current Values of the Optical Constants of H_2O(l) at 25°C between 15,000 and 1 cm^{-1}. *Applied Spectroscopy*, **50,** 1047-1057.

Donlon, C., I. Robinson, K. S. Casey, J. Vazquez-Cuervo, E. Armstrong, O. Arino, C. Gentemann, D. May, P. LeBorgne, J. Piollé, I. Barton, H. Beggs, D. J. S. Poulter, C. J. Merchant, A. Bingham, S. Heinz, A. Harris, G. Wick, B. Emery, P. Minnett, R. Evans, D. Llewellyn-Jones, C. Mutlow, R. W. Reynolds, H. Kawamura, and N. Rayner, 2007: The Global Ocean Data Assimilation Experiment High-resolution Sea Surface Temperature Pilot Project. *Bulletin of the American Meteorological Society*, **88,** 1197-1213.

Donlon, C. J., P. J. Minnett, C. Gentemann, T. J. Nightingale, I. J. Barton, B. Ward, and J. Murray, 2002: Toward improved validation of satellite sea surface skin temperature measurements for climate research. *Journal of Climate*, **15,** 353-369.

Fairall, C., E. Bradley, J. Godfrey, G. Wick, J. Edson, and G. Young, 1996: Cool-skin and warm-layer effects on sea surface temperature. *Journal of Geophysical Research.*, **101,** 1295-1308.

Gentemann, C. L. and P. J. Minnett, 2008: Radiometric measurements of ocean surface thermal variability. *Journal of Geophysical Research*, **113,** C08017.

Gentemann, C. L., T. Meissner, and F. J. Wentz, 2010: Accuracy of Satellite Sea Surface Temperatures at 7 and 11 GHz. *Geoscience and Remote Sensing, IEEE Transactions on*, **48,** 1009-1018.

Gentemann, C. L., P. J. Minnett, P. LeBorgne, and C. J. Merchant, 2008: Multi-satellite measurements of large diurnal warming events. *Geophysical Research Letters*, **35,** L22602.

Hanafin, J. A., 2002: On sea surface properties and characteristics in the infrared. Ph.D., Meteorology and Physical Oceanography, University of Miami, 111 pp.

Hanafin, J. A. and P. J. Minnett, 2001: Profiling temperature in the sea surface skin layer using FTIR measurements. *Gas Transfer at Water Surfaces.*, M. A. Donelan, W. M. Drennan, E. S. Saltzmann, and R. Wanninkhof, Eds., American Geophysical Union Monograph, 161-166.

Katsaros, K. B., W. T. Liu, J. A. Businger, and J. E. Tillman, 1977: Heat transport and thermal structure in the interfacial boundary layer measured in an open tank. *Journal of Fluid Mechanics*, **83,** 311-335.

Kent, E. C. and P. K. Taylor, 2006: Toward Estimating Climatic Trends in SST. Part I: Methods of Measurement. *Journal of Atmospheric and Oceanic Technology*, **23,** 464-475.

Minnett, P. J., 2003: Radiometric measurements of the sea-surface skin temperature - the competing roles of the diurnal thermocline and the cool skin. *International Journal of Remote Sensing*, **24,** 5033-5047.

Minnett, P. J., M. Smith, and B. Ward, 2011: Measurements of the oceanic thermal skin effect. *Deep Sea Research Part II: Topical Studies in Oceanography*, **58,** 861-868.

Ohring, G., B. Wielicki, R. Spencer, B. Emery, and R. Datla, 2005: Satellite Instrument Calibration for Measuring Global Climate Change: Report of a Workshop. *Bulletin of the American Meteorological Society*, **86,** 1303-1313.

Price, J. F., R. A. Weller, and R. Pinkel, 1986: Diurnal cycling: observations and models of the upper ocean response to diurnal heating, cooling and wind mixing. *Journal of Geophysical Research*, **91,** 8411-8427.

Soloviev, A. V. and P. Schlüssel, 1994: Parameterization of the cool skin of the ocean and of the air-ocean gas transfer on the basis of modeling surface renewal. *Journal of Physical Oceanography*, **24,** 1339-1346.

Swift, C. T., 1980: Passive microwave remote sensing of the ocean—A review. *Boundary-Layer Meteorology*, **18,** 25-54.

Ward, B., 2006: Near-Surface Ocean Temperature. *Journal of Geophysical Research*, **111,** C02005.

Wilheit, T. T., A. T. C. Chang, and A. Milman, 1980: Atmospheric Corrections to Passive Microwave Observations of the Ocean. *Boundary-Layer Meteorology*, **18,** 65-77.